

**FOURTEENTH EUROPEAN ROTORCRAFT FORUM**

**Paper No. 66**

**A NEW WIND TUNNEL TEST RIG FOR HELICOPTER TESTING**

**M. Stephan - V. Klöppel  
MESSERSCHMITT-BÖLKOW-BLOHM GMBH GMBH  
Munich, Germany**

**H.-J. Langer  
DEUTSCHE FORSCHUNGS- UND VERSUCHSANSTALT  
FÜR LUFT- UND RAUMFAHRT  
Braunschweig, Germany**

**20. - 23. September, 1988  
MILANO, ITALY**

**ASSOCIAZIONE INDUSTRIE AEROSPAZIALI  
ASSOCIAZIONE ITALIANA DI AERONAUTICA ED ASTRONAUTICA**

## A NEW WIND TUNNEL TEST RIG FOR HELICOPTER TESTING

M. Stephan - V. Klöppel  
MBB GmbH, Postfach 801140, D-8000 München 80, West-Germany

H.-J. Langer  
DFVLR, Flughafen, D-3300 Braunschweig, West-Germany

### **ABSTRACT**

This paper describes the steps taken to build up and to test a new Modular Wind Tunnel Model (MWM).

The MWM was scaled for 4 m rotors, i.e. that the available power, hub loadings, and dimensions of the main module meet the requirements for wind tunnel tests with future helicopters.

Definition and design of the different modules will be described. Emphasis is given to the basic module discussing different parameters to be taken into account so that the module fits into small fuselage models as well as in wide bodies.

The design of the model had to consider the different test environments as helicopter models will be tested in different test sections (e.g. "open" and "closed") of the DNW. Different ways to mount the module were studied so that interference effects and the system's dynamic behavior will not strongly restrict the test envelope.

Holding the blade tip Mach number constant under all power conditions demands a quick and accurate drive motor control. It will be shown, that a hydraulic power source can meet this demand. Accuracy of the swashplate control and shaft tilt is essential as an excellent repeatability of all control angles must be guaranteed.

For performance tests it is necessary to measure the hub loads; therefore a six component balance is integrated in the module. Design aspects, calibration, and results of this balance will be presented.

Data handling and improvements in monitoring the test results have been an important part during MWM pre-tests. Methods and procedures will be discussed.

In order to check the accuracy of the MWM-measurement data, wind tunnel results from previous tests will be shown using the same rotor mounted on a vertical rotor test stand.

## 1. INTRODUCTION

The development of new fixed-wing aircraft includes extensive windtunnel testing campaigns to reduce the risks and costs as well as the duration of the programs concerned. In helicopter development, systematic windtunnel testing has played a moderate role despite considerable uncertainty as to aerodynamic and flight-mechanical designs and calculations.

In future, too, flight tests will be used for the final testing of new aircraft and for verifying system characteristics. However, quite a number of data which has so far been collected by means of flight-testing may be supplied by windtunnel tests as well. Moreover, windtunnel testing provides data which cannot be supplied by flight tests.

As a consequence, future helicopter development programs must focus more intensely on exploring the possibilities offered by windtunnel testing.

This requires availability of the necessary testing technology and a reduction in present uncertainties regarding the possibilities of applying data collected in windtunnel tests to the production aircraft.

The technology has now been provided in the form of the "Modular Windtunnel Model" (MWM) described herein (see fig. 1.1). A projected follow-up program (validation program) will examine the possibilities of applying data gathered in testing helicopter models in the wind-tunnel to the production helicopter.

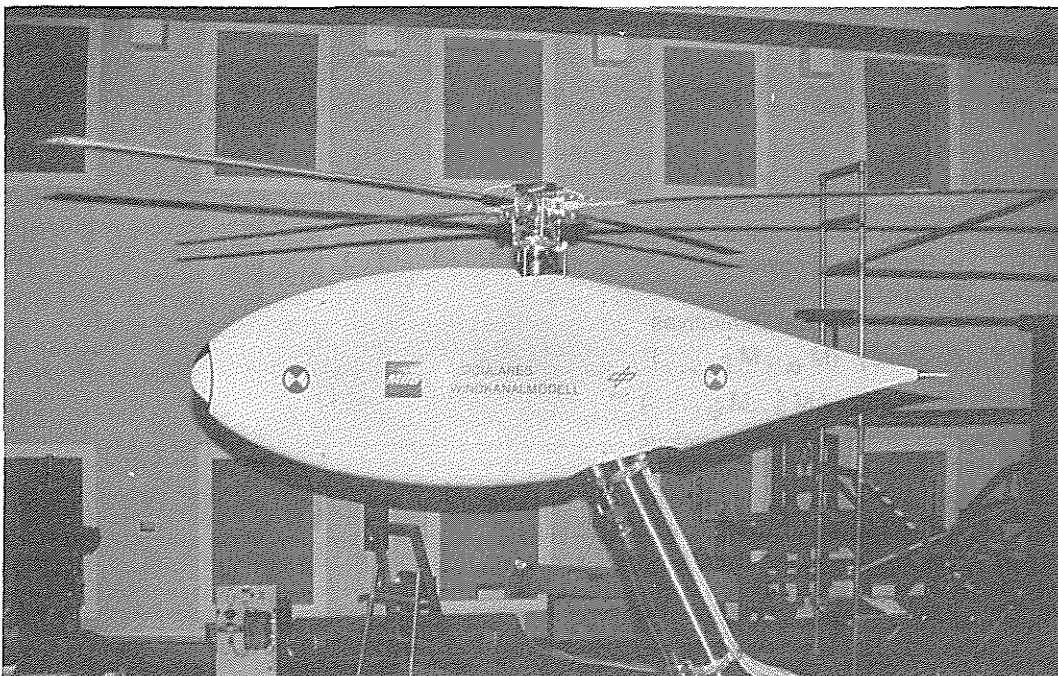


Fig. 1.1 Modular Windtunnel Model

The main similarity parameter of the MWM is the blade tip Mach number. The scaling factor, describing the ratio of model and full scale dimensions is  $s = 2,46$ . The similarity relation of all important physical properties is shown in Table 1.1.

The model system permits basic technological research as well as ongoing project-related research. The latter is to provide an optimal helicopter design regarding flight performance, flight characteristics, ease of operation, economy and mission capability.

As the model system is further developed, the aspects specified in Table 1.2 may be tested experimentally.

PHYSICAL PROPERTY	SCALING FACTOR	$S^N = \frac{\text{Full scale property}}{\text{Model property}}$
Blade Tip Mach Number		1
Advance Ratio		1
Disc Loading		1
Force		$S^2$
Frequency		$S^{-1}$
Froude No.		$S^{-1}$
Linear Dimensions		1
Linear Velocity		1
Lock No.		1
Per Rev. Frequencies		1
Power		$S^2$
Strain		1

Table 1-1: Similarity Relation of Important Physical Properties ( $S = 2,46$ )

- Interference Phenomena
  - o Rotor — Fuselage / Tail / Wings
  - o Rotor — Engines
- Performance
- Flightmechanical Derivatives
  - o Steady ( $M_{\alpha}, M_{\beta}, \dots$ )
  - o Dynamic ( $M_{\dot{\theta}}, M_{\dot{\psi}}, \dots$ )
- New Helicopter Configurations
- Flight in and out of Ground Effect
- Internal Aerodynamic ( Engine inlet, Nozzle)
- Higher Harmonic and Single Blade Control
- Noise

Table 1.2: Research Areas of the Modular Wind Tunnel Model

## 2. REQUIREMENTS

The windtunnel model is to be suitable for all present and future MBB helicopters and is to provide the most accurate data possible with respect to rotor forces and moments. The helicopters to be tested range from the small BN-109 to the medium-sized transport helicopter LTH (NH 90). The design affecting thrust, mast moment and drive torque comprises a correspondingly wide range (see Table 2.1).

Type	Main Rotor							Tail Rotor						Total System	
	Dia- meter	Chord	RPM	Blade Tip Speed	max. Thrust $C_T \sigma = 0,2$	Power (Gear Box Limit)	Torque	Dia- meter	Number of Blades	Chord $x=0,7$	RPM	Blade Tip Speed	Hover ISA SL with 25m/s cross wind	Gross weight	Maximum Cruise speed
Dim.	m	m	1/min	m/s	kN	kW	kNm	m	-	m	1/min	m/s	kW	kg	km/h
PAH2	13	0,5	316	215	148	1340	40,5	2,7	3	0,25	152	215	130	5000	250
TTH	16	0,6	257	215	217	2300	85,6	3,2	4	0,26	1235	207	170	8500	300
ALH	12,8	0,44	326	218,4	132	1320	38,7	2,7	4	0,38	1485	210	124	4000	290
BO 108	10	0,27	413	216	63	432	10	1,9	2	0,2	2114	210	60	2100	280
BK 117	11	0,31	383	220,8	81	632	15,8	1,9	2	0,18	2169	216	70	1200	245
BN 109	8,4	0,27	473	209	37	200	4	1,4	2	0,16	2675	196	30	3200	200
BO 105	9,87	0,27	424	218	62	515	11,6	1,9	2	0,18	2220	220	67	2400	270
NFH	16	0,6	257	215	217	2300	85,6	3,2	4	0,26	1235	207	170	9000	286

Table 2.1

In view of the variety of fuselage configurations of the various model sizes and the corresponding performance requirements, the system must be of modular design to meet the demanding requirements placed upon it. The system's suitability for universal application has been achieved by implementing the following design characteristics:

- The modular design, allowing the easy installation and replacement of
  - o The rotor shaft (without disassembly of the gear box)
  - o The fuselage covering and supplementary wings, connectable to the central module by a 6-component balance
  - o A tail rotor module with variable distance to the main rotor (see Fig. 2.1)
- A central module fitting all helicopter types in question and including drive, rotor controls and data transfer unit
- The model suspension on a rear sting ( see fig. 2.1 ) with the advantages of
  - o A largely undisturbed fuselage flow
  - o A possible running of the model in the open wind tunnel section

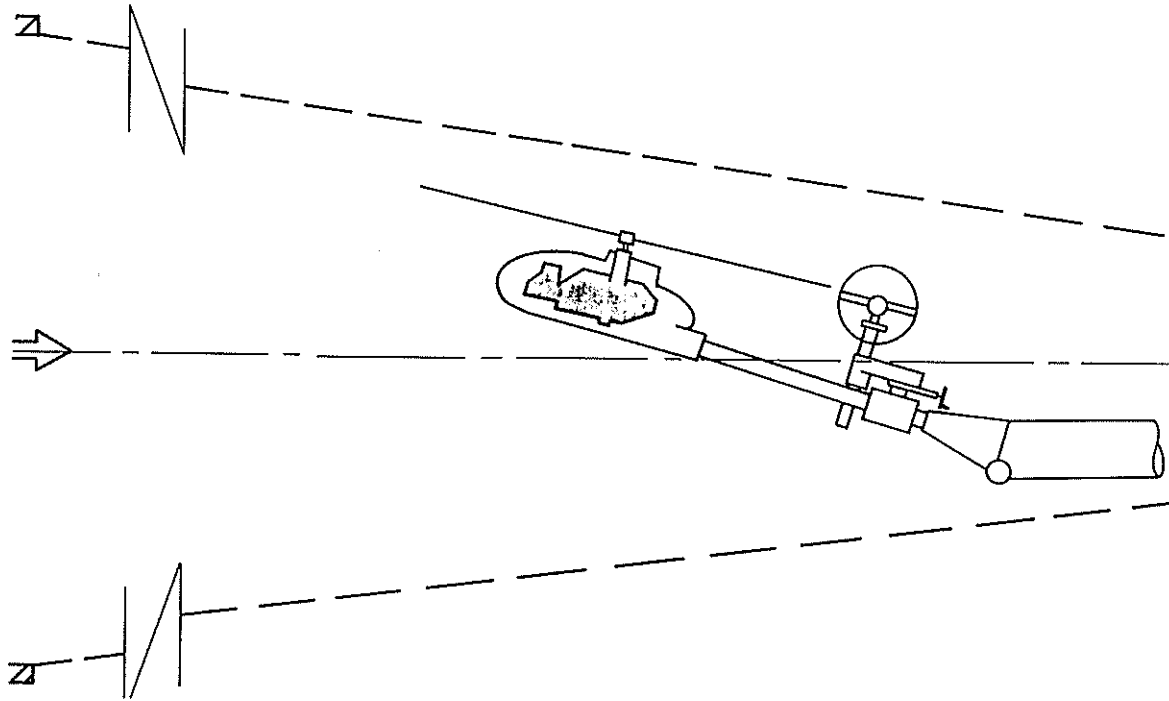


Fig. 2.1: Model Suspension Configuration with Tail-rotor

The model's rotor diameter decisively affects the dimensional base data. This aspect leads to the appropriate scale factors as regards the dimensions, the drive and the measuring devices. The model's rotor diameter must meet the following basic requirements:

- A Reynolds number as close as possible to the full scale Reynolds number
- Compatibility with the chosen wind tunnel with respect to
  - o Maximum velocity (convenient cross section)
  - o Minimum wall interference effects/avoidance of flow break down

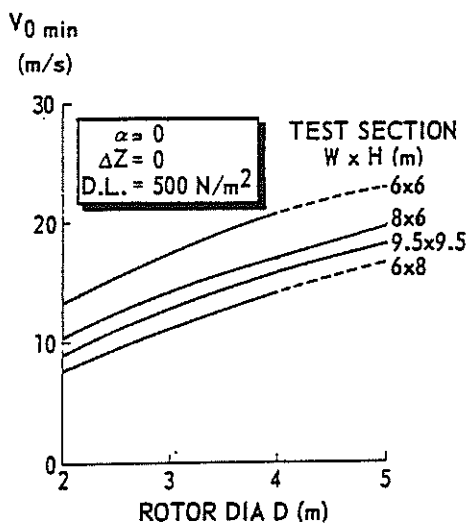


FIG. 2.2a MINIMUM ALLOWABLE WIND SPEED AT FLOW BREAKDOWN ONSET

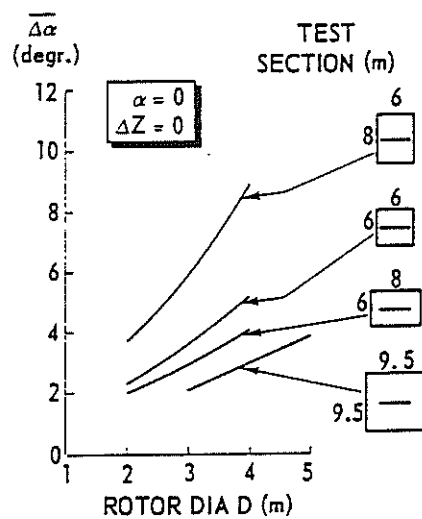


FIG. 2.2b AVERAGE INCIDENCE CORRECTION  $\overline{\Delta\alpha}$  FOR A ROTOR AT FLOW BREAKDOWN ONSET

As the model is run in the DNW with advance ratios up to  $\mu = 0,45$  the appropriate test section is the  $8 \times 6 \text{ m}^2$  section with a maximum velocity  $V_{\text{max}} = 110 \text{ m/s}$  (without model). The chosen model rotor diameter is  $D = 4 \text{ m}$ . The compatibility of this diameter with the  $8 \times 6 \text{ m}^2$  test section can be derived from the relatively low values of

- The minimum allowable wind speed (see Fig. 2.2 a)
- The average shaft incidence correction (see Fig. 2.2b)

at flow break down onset.

Depending on the chosen rotor diameter, the helicopter models to be used range from 2.1 to 3.75 in scale. Thrust, performance and torque are specified in Table 2.1.

### 3. SYSTEM DESIGN (mechanical part)

The system design focused primarily on

- model support (sting)
- choice of motor and motor accommodation
- choice of gear
- design of balance

As all subsystems are more or less dependent on one another, a total of 24 variants has been established and examined. The chosen configuration is depicted schematically in Fig. 3.1:

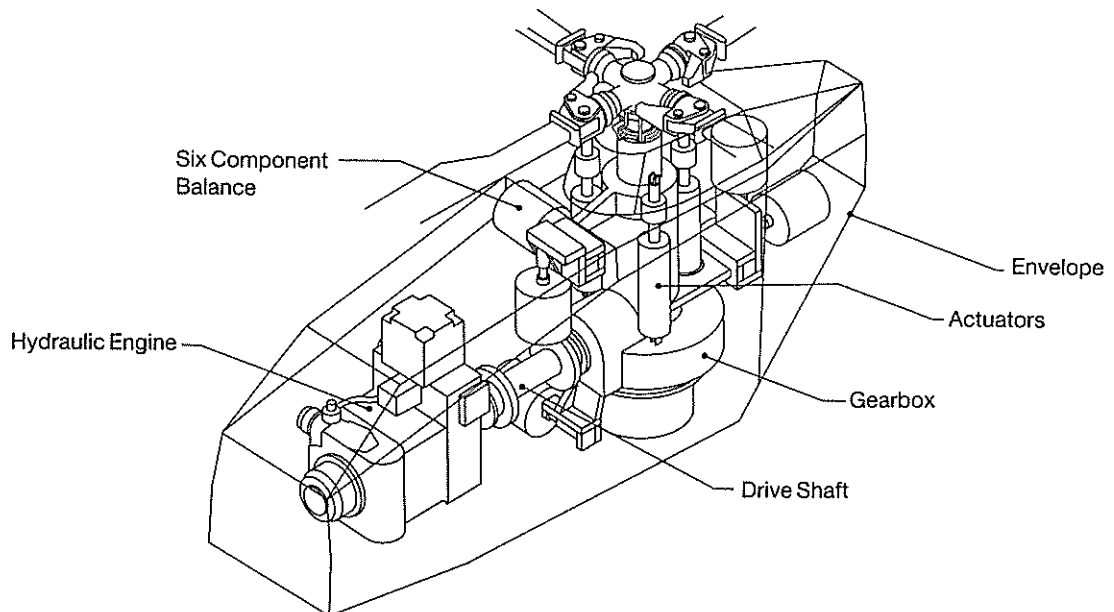


Fig. 3.1: Main Components

- A fixed system serving as the supporting structure for all assemblies, which is held in place by the model supporting (sting) and is firmly attached to the "DNW sting support".
- The model core comprising the rotor, the mast, the swash-plate, the actuators for pitch control, the gear box and the PCM system. The core is attached to the fixed system via six balance elements.
- The fuselage module mounted to and enclosing the fixed system. The mounting will in future also be in the form of a balance, which in contrast to the fixed system will permit measuring the fuselage forces as well.

Fig. 3.2 shows the operational windtunnel model. The sting is attached to a support system, which may be varied in height and is capable of allowing the model to pitch.

Fig. 3.3 depicts the open system and shows the components installed inside.

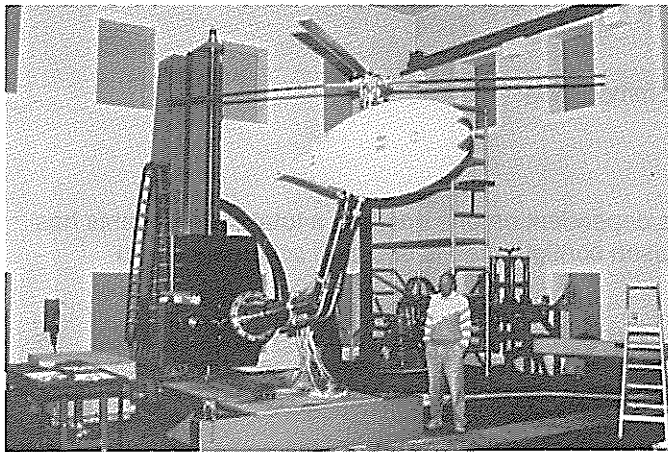


Fig. 3.2

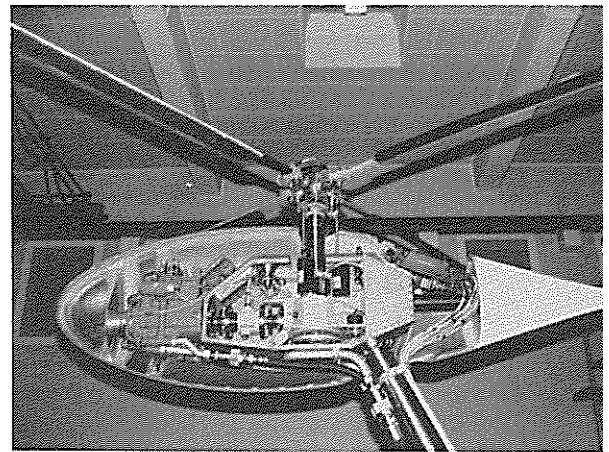


Fig. 3.3

### 3.1 Choice of subsystems

- Model support (sting)

Of the many support options available, a "downward and inclined" version was selected. This not only made it possible to use the movable DNW sting, it also resulted in the selected configuration being judged the best alternative under the given circumstances as far as aerodynamic characteristics were concerned.



- Choice of motor

The question as to which motor should be used depends primarily on the motor's speed accuracy under load. Following an abrupt change in torque by 50 percent, speed must be adjustable within 3 seconds to its nominal value without any over- or undershooting, within a tolerance of + 2 percent. Pneumatic, hydraulic and electrical drives were compared with respect to their performance, weight, size, necessary gear ratio, speed accuracy, and price. The optimal choice is a hydraulic motor: the specific volume/ performance characteristics are very good, and since its speed is relatively low, it provides a simple and inexpensive gear. Its dynamic characteristics are excellent due to the low inertial moment of the rotating parts. The motor selected was an adjustable axial piston engine (see fig. 3.4).

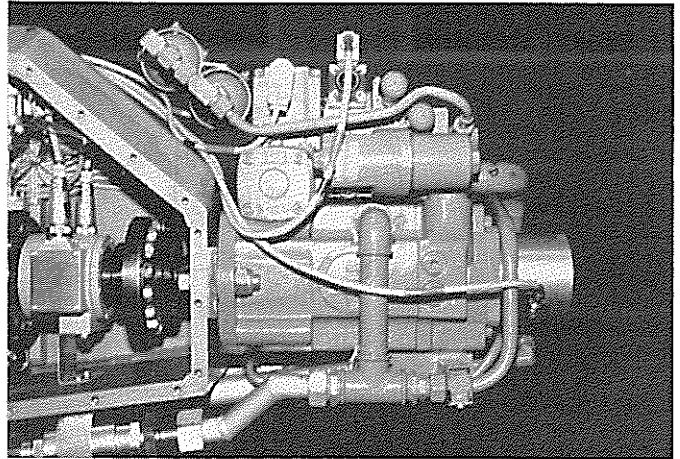


Fig. 3.4

- Gear

The selected bevel gear offers optimal assembly and maintenance as well as access to all aggregates contained in the module frame. This particular gear produced additional roll moments acting on the balance elements via the drive, but this is only a minor drawback when viewed within the overall context. The practical advantages mentioned above, especially costs, are quite preferable to a completely roll-decoupled drive concept.

- Balance

The rotor balance has to measure the six steady and dynamic rotor loads in a room, prescribed by the internal model frame (see fig. 3.1). This task requires a minimum of six balance components. The advantage of not exceeding this number can be deducted from:

- o The defined suspension, which leads to a proper decoupling of the different loads and prevents measurement failures due to temperature induced strains between the flexible primary and the rigid secondary part of the balance.

- o A low space requirement and the opportunity to implement large distances between the different balance elements.

On behalf of the gear box performance losses the measurement of the motor torque is necessary in addition to the balance torque.

The balance elements should measure forces only along one defined axis, being decoupled from supplementary moments.

For the segregation of rotor and airframe loads a separate 6-component airframe balance at the rear end of the central module is planned (see fig. 3.5). It's working principle is the same as that one of the rotor. A tail rotor can be suspended separately on the model sting having its own balance. (See fig. 2.1).

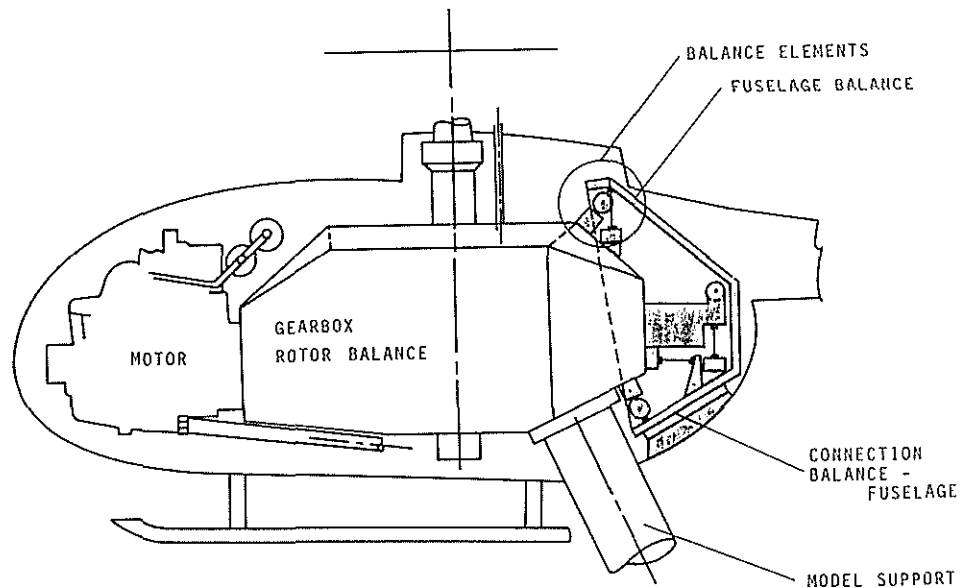


Fig. 3.5: Fuselage Balance

#### 4. DESCRIPTION OF THE ASSEMBLIES

##### 4.1 Fixed system

###### 4.1.1 Sting

The sting connects the windtunnel model with the model support. It supports the entire model and bears the rotor forces and moments (see fig. 3.2). In addition, the sting is used to carry the supply lines of the hydraulic motor and the electrical lines for energy supply and signal transmission. The sting consists of two parts and is hollow to avoid excess weight.

###### 4.1.2 Casing

The upper end of the sting holds the model's casing, which is fastened with screws. This is a welded structure made of several aluminium plates. The casing is closed by two plates screwed onto it and additionally fastened by pins.

The bottom of the casing holds the hydraulic lines to the hydraulic motor, which is flanged directly to the casing (see fig. 4.1).

##### 4.2 Model core

###### 4.2.1 Transmission of drive moment

The drive moment is transmitted to the core via a Thomas coupling. A bevel gear step redirects the drive moment by 90 degrees (see fig. 4.2). Speed is geared down by a ratio of 1 : 2.22. An even ratio has been avoided to exclude any coupling of the harmonic vibrations of the motor shaft and the rotor mast.

#### 4.3 Balance for the model core

The rotor balance consists of individual balance elements which can bear only tension/compression forces. In lateral force direction, they are very flexible due to two beryllium elements, which feature a very low elastic modulus as compared to steel (see fig. 4.2). This pronounced flexibility also considerably reduces the transmission of torsion and bending moments. The normal forces within the balance elements are measured with load cells. The only "force" which crosses the boundary between the fixed system and the model core is the drive moment which is transmitted to the bevel gear by the hydraulic motor. The force of this moment is determined via a torque tube (see fig. 4.2). In addition, provision must be made to prevent the drive shaft from causing any longitudinal or lateral forces or bending moments to be transmitted between the fixed system and the core. To this end, the torque tube is suspended between two Thomas couplings, which are very flexible both in axial and bending direction.

The upper mast bearing is a four-point bearing, which also takes up the rotor thrust. This arrangement allows a relatively simple replacement of the rotor mast, as the bottom bearing presents only a radial support, and the gear setting is not affected by the mast assembly.

#### 4.4 Transmission of the measurement signals

Measurement signals from the rotating system are transmitted to the fixed system by a slip ring. A slip ring body with 12 silver rings is used. Prior to transmission at the slip ring, the signals are digitized in a PCM system, which rotates synchronously with the rotor speed (see fig. 4.2).

#### 4.5 Rotor control

The rotor is controlled via three electrodynamic actuators, the position of which is set off against the axis of the mast by an angle of 120 degrees. The cylinders represent electromechanical linear drives which produce a regulated linear movement. Each drive is equipped with a low-friction precision spindle driven by a controlled DC motor and thus produces a regulated linear movement. Various feed-back converters integrated in the cylinder supply the system's control unit with data on the motor current, speed and position. The system's force, speed and position can therefore be programmed (see fig. 4.2).

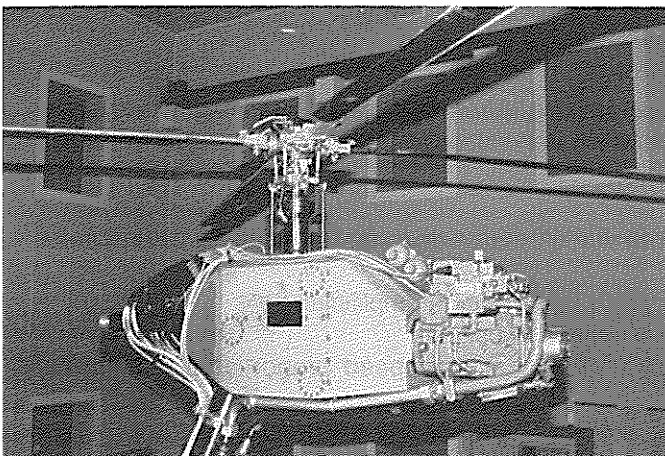


Fig. 4.1

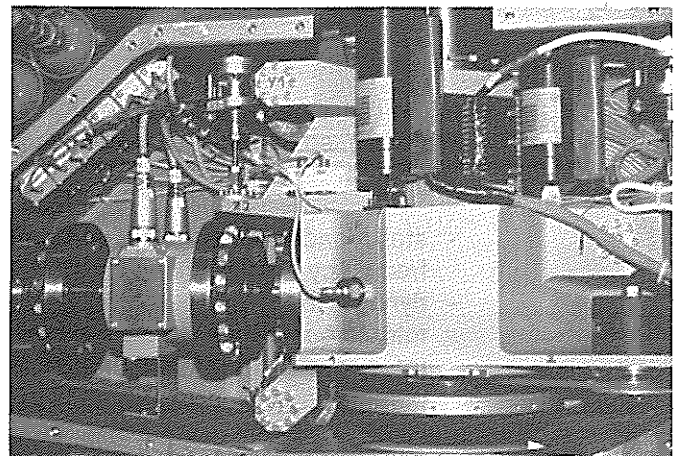


Fig. 4.2

## 5. MEASURING SYSTEM

In correlation of the values to be measured a number of sensors are installed in the model (see fig. 5-1). Depending on their position, sensors are called to be in the 'rotating system' or in the 'fixed system' of the MWM (fig. 5.-2).

When tests are performed in the wind tunnel, there are pressure and temperature sensors in addition. As the MWM is sting mounted, the location of the model, i.e. the hub position relatively to the test section walls, and the models' angle of incidence is measured, too.

### 5.1 Sensors in the "rotating system"

34 sensors mostly of the strain gauge type are installed (fig. 5.-2). The voltage level of such sensors are quite low. In order to avoid jamming it is necessary to amplify the signals as near as possible at the sensor location. Therefore 32 amplifiers (amplification factor between 1 and 10 000) are located on the rotor hub.

Analog data transfer from the rotating to the fixed system demands several slip rings. As room is very limited in the MWM, it was decided to use a PCM (pulse code modulation) data transfer unit which produces a serial-digital data stream not sensitive to electric interference from other sources.

All sensor signals pass 240 Hz filters as a 140Hz resolution of each signal is required aliasing-free. 140Hz matches the 8th harmonic of a 4m Mach-scaled rotor.

Due to filtering, all signals get a constant phase shift which is corrected either by software (the magnitude of the phase shift is determined by calibration) or by use of the rotor azimuth saw tooth signal as a reference. This signal is sent from the 'fixed system' via slip ring to the 'rotating system', then filtered and sent back via the PCM unit to the ground.

All sensor signals have to be adapted to the expected maximum and minimum voltage level. It is therefore necessary to know offset and amplification prior to the tests, as the modification of these two values means hardware modification on resistance and potentiometer set up.

### 5.2 Sensors in the "fixed system"

The sensors located in the 'fixed system' use different physical measuring principles (fig. 5.-2), so that an individual signal conditioning is necessary. Some principles are explained briefly:

- static loads on the balance are measured via 'off the shelf' force transducers using carrier frequency amplification;
- dynamic loads are measured via piezo crystals using charge amplification;
- rotor torque is measured via a strain gauge using a FM signal;
- rotor revolution is measured inductively and transmits a speed proportional rectangular potential.

The data are being fed into a data distribution device (crossbars distributor) after signal conditioning of the sensors in the "fixed system" and after decoding the PCM signal from the "rotating system" (fig. 5.3). The output of this distributor is used for quick look. The signals can be displayed online on a CRT in the time domain or in the frequency domain using a frequency analyser.

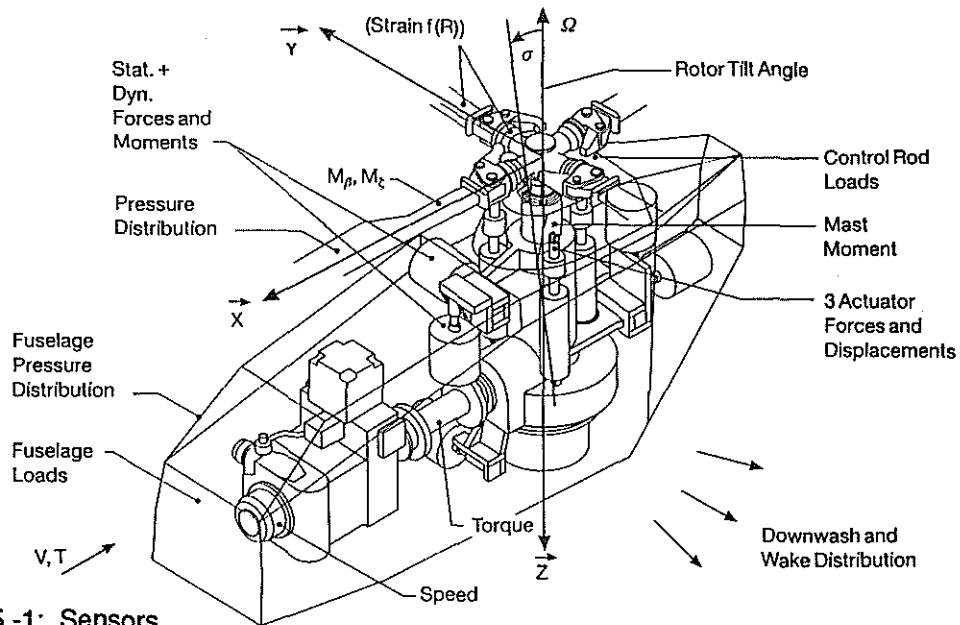


Fig. 5.-1: Sensors

	Sensor	measured by...	number
fixed system	rotor balance:static loads	strain gauge	12
	rotor balance:dynamic loads	piezo crystal	6
	swashplate actuator	potentiometer	3
	shaft tilt	inclinometer	1
	rotor torque	strain gauge	1
	rotor revolution	inductive	1
	analog azimuth angle	saw tooth potentiometer	1
	digital azimuth angle	optical	1
	acceleration	piezo crystal	3
	temperature	semi conductor	19
rotating system	blade flap lag torsion	strain gauge	24
	mast moment	strain gauge	4
	blade pitch	potentiometer	2
	pitch link:static loads	strain gauge	2
	pitch link:dynamic loads	piezo crystal	2

Fig. 5.-2: Table of sensors used in the MWM

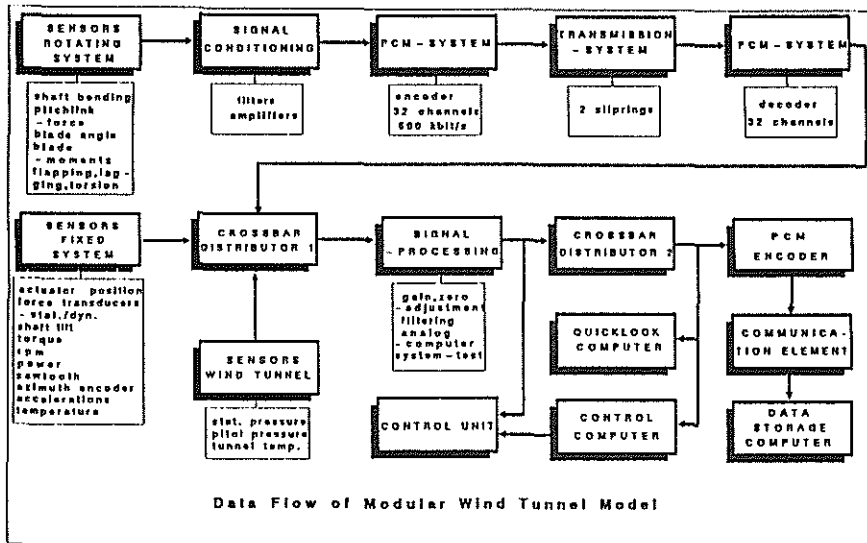
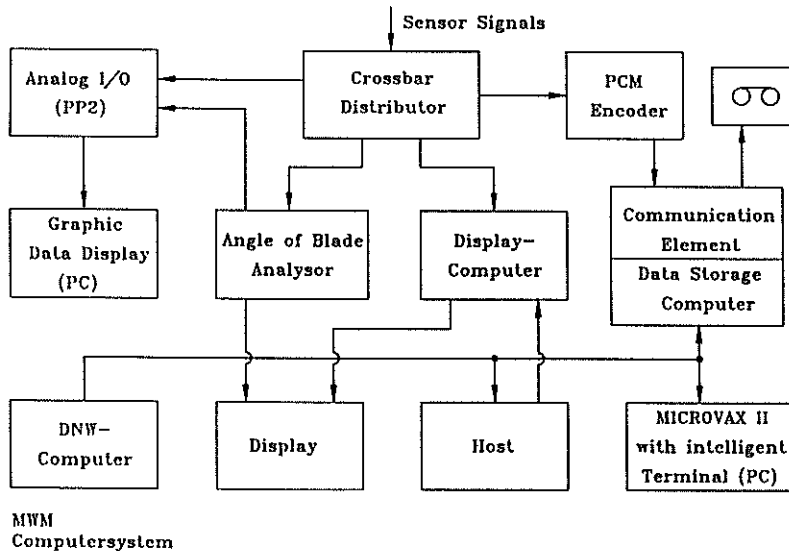


Fig. 5.-3

## 6. DATA PROCESSING

Data processing is done with four process computers in connection with different peripheral devices (fig. 6.-1)



MWM  
Computersystem

Fig. 6.-1

After the adaption of the sensors voltage level, some data are fed into an I/O device allowing the display of static data on a PC screen and printer.

Other data are used as MWM status indicators, e.g. blade pitch sensor (for the actual collective and cyclic pitch), thrust coefficient, mast bending moment, etc. These data are displayed on the control panel located in the near by container.

Furthermore all sensor signals pass a PCM encoder and a so-called 'communication element'. Latter can be seen as an interface between the serial PCM data stream and the data storage computer (LSI 11/23). For offline data processing the raw data are stored on a digital tape for about 1.2 seconds (equivalent to 21 rotor revolutions).

A print out of all sensor signals of one rotor revolution is optional, mostly used as a good reference to other signals or data points and to detect sensor defects.

Data reduction is done by data shifting from the time domain to the frequency domain using a Micro-VAX II. Only data which are of interest for further data evaluation are stored:

- static values (0/rev)
- dynamic values (1/rev, 2/rev, 3/rev, 4/rev, 5/rev, 8/rev).

Besides the most common VT100 and Tektronix 4015 terminals, an Apple Macintosh PC is connected to the VAX either via Ethernet or directly via a serial port. Applying a VT100 terminal emulation software makes it possible to copy specific data from the VAX to different MAC application programs (data management, spreadsheet, graphic, text, etc.). This is a very handy and effective method for quick look and off line data evaluation, because application programs for PC's are quite comfortable,

The data of the DNW computers are transferred via Ethernet to the data storage computer (performing the print out of one rotor revolution and writing the data to the mag. tape).

## 7. CALIBRATION PROCEDURES

### 7.1 Rotor Balance

Primarily this balance measures the static loads, but dynamic loads can also be determined; however, due to the lack of accurate calibration procedures, dynamic loads can only be used comparatively or qualitatively.

Two different calibration methods can be applied:

- If the loads measured at the balance force transducers do not interfere with each other, i.e. that the crosstalk of the load cells is negligible only three forces and moments are necessary to find out the calibration matrix, when they are applied at the rotor hub one after each other. This matrix can be assumed to be linear and all elements which are not directly related to the hub load direction and the balance force transducer can be neglected.

- In the non-ideal case it is necessary to pre-load the balance in the expected range of loadings. The calibration procedure is quite time consuming, because all expected load combinations must be calibrated. As each force or moment is related to several combinations, the number of matrix elements is enormous. Fortunately some combinations need no calibration in both directions, e.g.  $F_z$  (thrust), and  $M_z$  (rotor torque), or the expected loads are small e.g.  $F_y$  (lateral hub force). Nevertheless calibration time increases considerably with the number of steps of added calibration masses.

The comprehensive calibration technique demands a special computer code for data evaluation. A Taylor series is used consisting of linear elements, quadratic elements, and combinations of both.

The higher the number of measurements (calibration points) the higher the accuracy of the balance. Test results showed that the accuracy of the hub load measurements is better than 1%.

Dynamic balance tests were performed by mounting the balance on a concrete block, so that measured resonance frequencies result from the balance and not from the support. A sweep test was accomplished in three directions using two electro dynamic shakers. Moments were applied by a 180° phase shift excitation of one shaker.

These tests do not take into account pre-loads, the influence of rotating parts, and the variation of input forces and moments. Dynamic response is measured via the piezo crystal washers mounted close to the force transducers.

### 7.2 Actuators And Pitch Angles

Three actuators are used to move the swashplate. Actuator displacement is measured by a linear potentiometer.

The desired pitch angle follows the equations:

$$[q] = [G] * [z]$$

$[q] = [q_0, q_s, q_c]^T$  - collective, long.cyclic, lat. cyclic [°]

$[z] = [z_1, z_2, z_3]^T$  - displacement of the actuators [mm]

$[G]$  is a quadratic 3 by 3 transfer matrix.

In case of the MWM geometry the equations can be assumed to be linear ( $1\text{mm} \approx 0.1^\circ$ ). This renders possible an analog computer to accomplish the conversion between control angle and actuator displacement. The results of the computed nominal rotor control angles are displayed at the control panel.

The softness of the control system is not considered in the calculation. To get the actual control angle, a FFT of the blade pitch sensor is accomplished using a specific designed  $\mu$ -processor. The blade pitch angle is calibrated using an inclinometer as a reference.

The difference between the actual and nominal control angles is shown in fig. 7.2-1 (notice the different scale of the diagrams!). It is evident that for the collective pitch only, the difference between the actual and nominal values are nearly constant, because collective pitch moves all actuators with the same magnitude in the same direction. The difference of the nominal and actual value of the longitudinal cyclic pitch depends on the magnitude of the collective pitch and on the magnitude of the longitudinal angle itself. In addition, a variation of one cyclic control angle causes a slight variation of the other two control angles.

This substantiates the necessity of a pitch angle control by a blade pitch sensor on the hub.

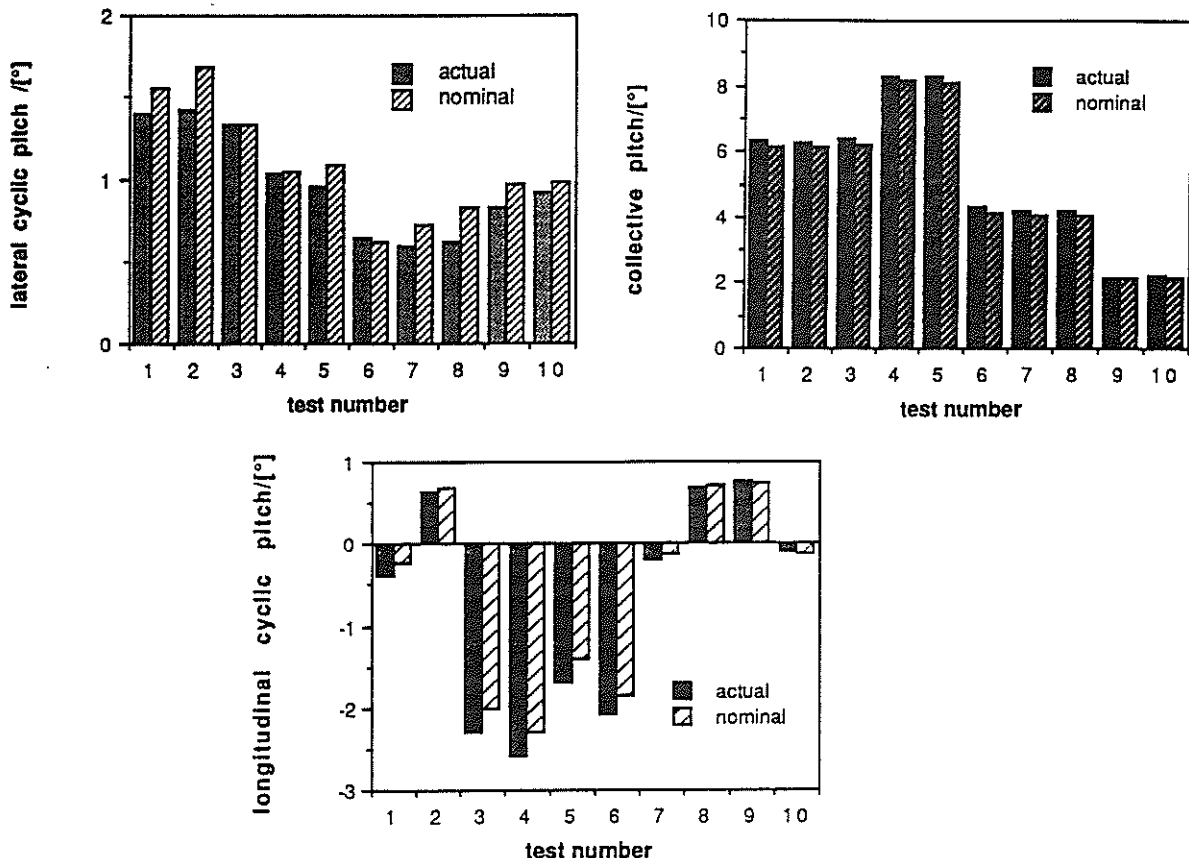


figure 7.2-1: Comparison of actual and nominal rotor control angle at  $\mu=0.1$  (open test section)



### 7.3 Other MWM Calibration Procedures

Before starting operation with the MWM, additional calibration or pre-checks had to be performed:

- ground resonance tests as described in reference /1/,
- vibration check at operational speed with a rotor/blade dummy mass,
- balance control of the whole rotating system.
- oil temperature in the gear box at different shaft tilts and their effect on sensors (offsets).

## 8. WIND TUNNEL TESTS

### 8.1 Test Program

The main part of the wind tunnel test program was established to investigate the accuracy of measurement with the MWM. The test procedure calls for variations of tunnel speed, collective pitch, cyclic pitch, and shaft tilt at constant tip Mach number.

The same test procedure was used for experiments with a proven rotor test stand (RoTeSt) in the same wind tunnel test section. (ref. /2/,/3/ ). Therefore results can be compared and accuracy can be evaluated.

In addition, the MWM was operated in two different test sections (8m x 6m, open; 8m x 6m, closed) to get an idea about the magnitude of wind tunnel interference effects influencing specific measured values, mainly static loads. Therefore care was taken to adjust the same rotor conditions in both test sections.

In order to match flight test conditions with wind tunnel test conditions different approaches were used:

>> collective pitch and velocity were adjusted for the MWM rotor as measured in flight or as calculated.

The rotor disc was tilted, so that the scaled thrust vector is equivalent to the flight condition. 1/rev flap was reduced to zero.

>> power and velocity were adjusted for the MWM rotor as measured in flight or as calculated.

The rotor disc was tilted as above.

### 8.2 Test Results

Fig. 8.2-1 shows the rotor torque measured with a torque meter and with the balance itself. Mainly three force transducers are involved in y-direction of the balance. The slope of the curve indicates the gear box ratio, as the hydraulic motor rotates about 2.2 faster than the rotor.

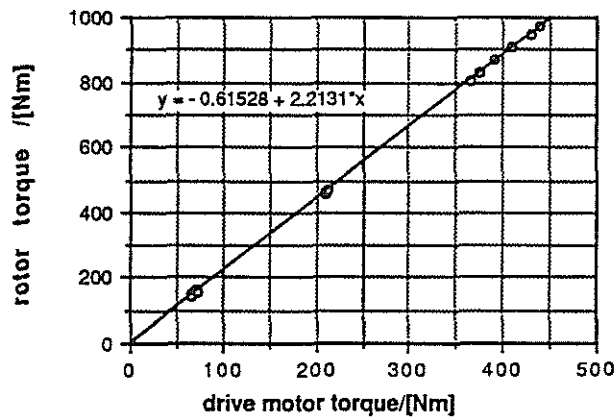


figure 8.2 -1: Reproducibility of measured values using the drive moment of the hydraulic motor and the balance measured rotor torque moment as an example.

Fig. 8.2-2 shows a plot of the first harmonic of blade flap versus the rolling and pitching moment at the balance. The correlation of these values can be used to check the accuracy of the balance. The offset of the data points from linearity is probably caused by a zero offset of the force transducers due to temperature related distortion. Oil cooling of the gear box was not sufficient for some test conditions esp. for tests with high shaft tilt angles. An oil-pump was installed to solve this problem.

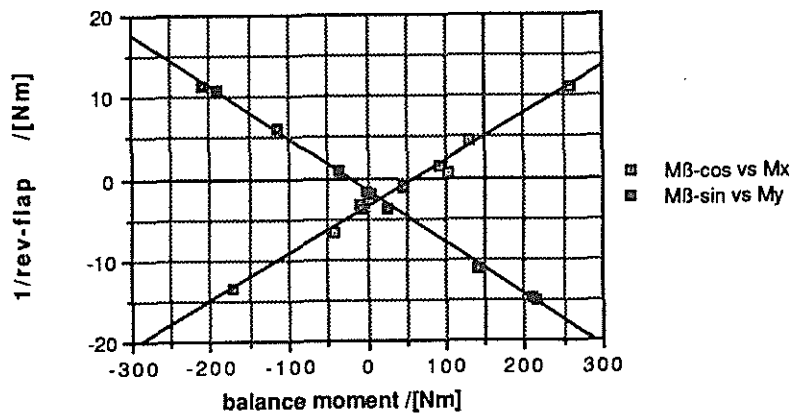


figure 8.2-2: Correlation of the rolling moment ( $M_x$ ) with the 1/rev-cos part of the flapping moment ( $M_\beta$ ) and pitching moment ( $M_y$ ) with the 1/rev-sin part of the flapping moment ( $M_\beta$ ).  $\mu=0.1$ ; 3700 N trimmed thrust.

Fig. 8.2-3 shows the accuracy of the hydraulic feed back control used to hold rotor speed constant. The actual speed is measured with the RPM sensor of the torque meter.

The accuracy of the data is better than 5 rpm (< 0.5%). Scatter can occur when the control vector ( $v_x$ ,  $a$ ,  $q_{coll}$ ,  $q_c$ ,  $q_s$ ) is varied and hub loading changes. Each symbol in the diagram stands for a specific rotor condition.

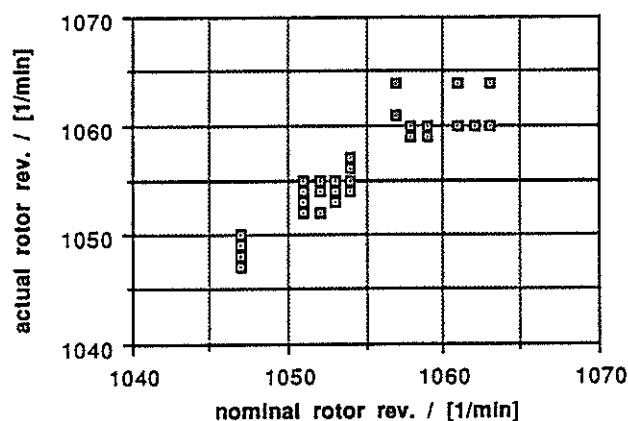


figure 8.2-3: Correlation between the actual and nominal rotor revolution for the MWM hydraulic drive system.

To ascertain the accuracy of the complete system, test results of the MWM were compared with those of the rotor test stand (RoTeSt) measured in the closed test section of the DNW (table 8.2-1). In addition MWM data were obtained in the open test section, in order to find out the wind tunnel interference effects.

To achieve a better distinctness, the data of table 8.2-1 were converted to diagrams. Figure 8.2-5 and Figure 8.2-6 show lateral hub force, thrust, pitch moment, roll moment, and torque for different advance ratios.

The offset between the test points of RoTeSt and MWM mainly arises from differences of the test conditions, (e.g. tunnel speed,  $\mu$ , and rotor revolution).

In addition, RoTeSt tests were accomplished using a downwash measurement device, installed on the wind tunnel floor. Due to wind tunnel flow interference this device affects mainly the rotor pitch moment ( $M_y$ ) and the torque esp. at higher tunnel speed. To quantify the different results more measurements must be considered.

When evaluating wind tunnel interference, only those results are of interest which are determined with the same model (MWM) in different test sections.

Calculations based on Heyson's code confirm, that the effective angle of disk path plane tends to 'nose up' for the closed test section and 'nose down' for an open test section. So wind tunnel interference does influence the angle of attack and in addition all other elements of the control vector i.e. dynamic pressure, and the rotor control angles /ref.4/. Further investigations are desirable to learn more about the interference between rotor and wind tunnel.

run-N <sup>o</sup>	v	$\alpha_{\text{shaft}}$	$\theta_{\text{coll}}$	$\theta_{\text{lat}}$	$\theta_{\text{long}}$	rpm	F <sub>x</sub>	F <sub>z</sub>	M <sub>x</sub>	M <sub>y</sub>	M <sub>z</sub>
RTS1095	21.8	-10.1	8.3	1	-2.5	1034	-108.3	-4875.1	510.5	170.1	602.5
O2M1095	21.2	-10.1	8.3	1.03	-2.56	1044	-103.27	-4552.51	441.54	54.99	623.34
C2M1095	22.4	-9.9	8.3	1.0	-2.6	1050	-100.98	-4923.8	495.03	141.61	618.94
RTS1093	21.8	-10.1	8.3	1	-1.6	1038	-195.1	-4939.8	450.7	433.1	590.3
O2M1093	21.7	-10.2	8.29	0.96	-1.66	1042	-194.97	-4585.38	365.63	289	609.96
C2M1093	22.1	-9.8	8.3	1.0	-1.7	1050	-196.54	-4961.3	416.72	377.86	605.38
RTS2097	42.2	-10.1	8.6	1	-4.6	1043	-128.2	-4549.2	293.3	59.3	578.1
O2M2097	44.6	-9.9	8.62	0.87	-4.69	1050	-125.09	-4472.39	348.08	-37.79	665.34
C2M2097	44.6	-9.9	8.6	0.9	-4.7	1054	-133.24	-4798.63	333.93	-34.74	658.88
RTS2100	42.1	-10.2	8.7	1.1	-5.6	1042	-39.1	-4350.5	320.4	-278	596
O2M2100	45.5	-10	8.72	0.95	-5.57	1052	-45.96	-4368.53	402.51	-283.08	684.34
C2M2100	44.7	-9.9	8.7	0.9	-5.6	1054	-47.28	-4667.44	387.94	-276.88	679.3
RTS2593	53.8	-10.1	8.6	0.6	-3.7	1054	-348.7	-4588.7	139.8	674.4	526.3
O2M2593	56.1	-10	8.6	0.61	-3.75	1054	-346.98	-4365.44	169.49	454.76	620.41
C2M2593	55.8	-9.8	8.6	0.61	-3.75	1054	-350.23	-4622.19	138.02	458.13	611.06

Table 8.2-1: Comparison of test data with different models in open and closed 8m by 6m test sections. RTS - Rotor Test Stand, closed test section; O2M - MWM open test section; C2M - MWM, closed test section.

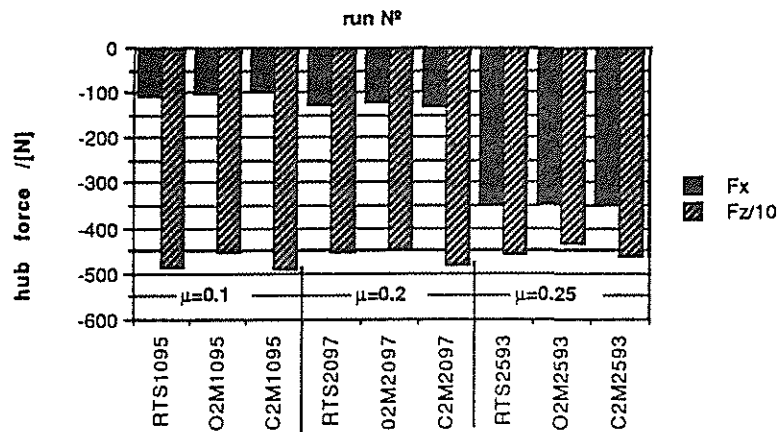


figure 8.2-5: Rotor balance measurements; hub forces (selected data points from table 8.2-1)

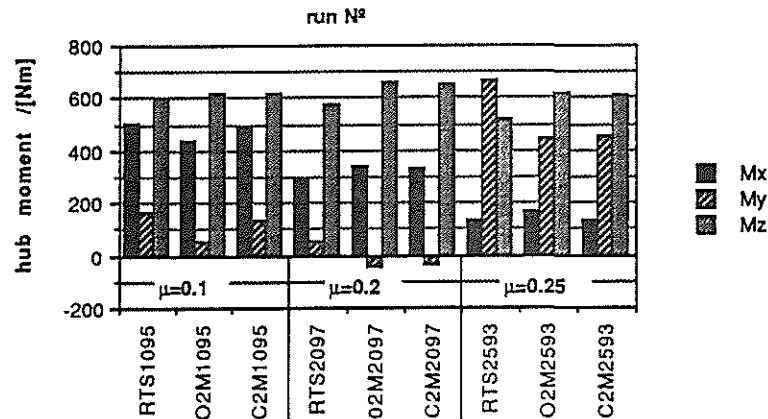


figure 8.2-6: Rotor balance measurements; hub moments (selected data points from table 8.2-1)

## 10. CONCLUSIONS

A Mach scaled wind tunnel model for the testing of a complete helicopter with a rotor diameter of  $D = 4$  m has been developed and successfully tested. The model will be used to test aerodynamic phenomena, especially interference effects and performance, flight mechanical problems, advanced rotor control and noise from main and tail rotor. These research objectives and the planned applicability for several helicopter types required a modular low volume design. The design requirements of good maintainability of the model and high accuracy of the rotor balance, the blade control pitch and the rotational rotor speed could be realized successfully. The precise rotor speed can be favourably controlled by a hydraulic drive system. The measurement data are transferred by a PCM system and analyzed, stored and displayed by an extensive digital system.

In order to validate the model with respect to the comparability of wind tunnel and flight tests, in the near future a program will start to test wind tunnel interference and similarity problems.

## 11. REFERENCES

- /1/ H.-J. Langer, F.Kiessling, R.Schröder: A model for wind tunnel rotorcraft research - ground resonance investigations. 2nd European Rotorcraft Forum, 1976
- /2/ P. Hamel et al.: Helicopter aeromechanic research at DFVLR; recent results and outlook. Vertica Vol.11, N°1/2, pp 93-108, 1987
- /3/ V. Mikulla et al.: Windkanaluntersuchungen zur aerodynamischen Optimierung von Rotorblättern der nächsten Generation. MBB UD-445/85
- /4/ H.-J. Langer: Aspects of wind tunnel interference effects on rotor model loadings. 13th European Rotorcraft Forum, paper n° 12.2, 1987
- /5/ M. Seidel, R.A. Maarsingh: Test Capabilities of the German-Dutch Wind Tunnel DNW for Rotors, Helicopters and V/STOL Aircraft. 5. European Rotorcraft Forum, Amsterdam, 1979